Pilot/Vehicle Analysis of a Twin-Lift Helicopter Configuration in Hover

R. A. Hess* and P. M. Tran†
University of California, Davis, Davis, California

A pilot/vehicle analysis of a twin-lift helicopter configuration carrying a load suspended from a rigid spreader bar is undertaken. The task is one of lateral/vertical control in hover. A two-pilot manual control structure is formulated in which the pilot of the "master" helicopter maneuvers his vehicle in response to internally generated position commands. The pilot of the "slave" helicopter senses master helicopter translational motion and uses it as a position command to his own vehicle. The required pilot equalization in all feedback loops is established using classical frequency domain pilot/vehicle analysis techniques based upon the crossover model of the human pilot. Closed-loop performance is assessed through computer simulation.

Nomenclature

F = aerodynamic/propulsive force in vehicle plane of symmetry, lbf
$F_{\dot{z}_M}, F_{\dot{z}_S}$ = stability derivatives $\partial F/\partial \dot{z}$ for master and slave vehicles, lbf·s/ft
$F_{\delta_{c_M}}, F_{\delta_{c_S}}$ = stability derivatives $\partial F/\partial \delta_c$ for master and slave vehicles, lbf/in.
$G_y, G_z, G_{\dot{z}}, G_\phi$ = pilot transfer functions
H_M, H_S = distance between vehicle center of gravity and tether attachment point for master and slave vehicles, ft
I_B = spreader bar polar moment of inertia, slug·ft^2
I_M, I_S = roll moment of inertias for master and slave vehicles, slug·ft
L_B = spreader bar length, ft^2
L_M, L_S = tether lengths for master and slave vehicles, ft
M = aerodynamic/propulsive rolling moment, ft·lbf
m_L = mass of the load, slugs
m_B = mass of the spreader bar, slugs
m_M, m_S = masses of master and slave vehicles, slugs
$M_{\delta_{a_M}}, M_{\delta_{a_S}}$ = stability derivatives $\partial M/\partial \delta_a$ for master and slave vehicles, ft·lbf/in.
$M_{\dot{\phi}_M}, M_{\dot{\phi}_S}$ = stability derivative $\partial M/\partial \dot{\phi}$ for master and slave vehicles, lbf·ft·s/rad
$M_{\dot{y}_M}, M_{\dot{y}_S}$ = stability derivative $\partial M/\partial \dot{y}$ for master and slave vehicles, lbf·s
xyz = coordinates in Earth-fixed reference frame, ft
y_B = y coordinate of spreader bar center of mass, ft
y_{c_M}, y_{c_S} = lateral position commands for master and slave vehicles, ft
y_L = y coordinate of load, ft
y_M, y_s = y coordinates of the centers of mass of master and slave vehicles, ft
z_B = z coordinate of spreader bar center of mass, ft
z_L = z coordinate of load center of mass, ft
z_{c_M}, z_{c_S} = altitude commands for master and slave vehicles, ft
$\dot{z}_{c_M}, \dot{z}_{c_S}$ = altitude rate commands for master and slave vehicles, ft/s [note: $\dot{z}_{c\_} \neq \mathrm{d}(z_{c\_})/\mathrm{d}t$]
z_M, z_S = z coordinates (altitudes) of master and slave vehicles, ft
$\delta_{a_M}, \delta_{a_S}$ = lateral cyclic pitch inputs from master and slave pilots, in. (measured at pilot's hand)
$\delta_{c_M}, \delta_{c_S}$ = collective pitch inputs from master and slave pilots, in. (measured at pilot's hand)
Δy = $y_M - L_B - y_s$, coordinate transformation used in obtaining decoupled equations of motion, ft
Δz = $z_M + z_S$, coordinate transformation used in obtaining decoupled equations of motion, ft
$\Delta\phi$ = $\phi_M - \phi_S$, coordinate transformation used in obtaining decoupled equations of motion, rad
ε_B = spreader bar inclination with respect to horizontal, rad
$\varepsilon_M, \varepsilon_S$ = tether line inclination with respect to vertical for master and slave vehicle, rad
ϕ_M, ϕ_S = roll attitudes of master and slave vehicles, rad
$\sum y$ = $y_M + y_S$, coordinate transformation used in obtaining decoupled equations of motion, ft
$\sum z$ = $z_M + z_S$, coordinate transformation used in obtaining decoupled equations of motion, ft
$\sum\phi$ = $\phi_M + \phi_S$, coordinate transformation used in obtaining decoupled equations of motion, rad
θ = angle between spreader bar and load cable, rad

Received Dec. 8, 1986; presented as Paper 87-0345 at the AIAA 25th Aerospace Sciences Meeting, Reno, NV, Jan. 12–15, 1987; revision received July 6, 1987.

*Professor, Department of Mechanical Engineering, Division of Aeronautical Science and Engineering. Associate Fellow AIAA.

†Graduate Student, Department of Mechanical Engineering, Division of Aeronautical Science and Engineering (currently, Aerospace Engineer, General Dynamics Corp., Pomona, CA).

Introduction

THE twin-lift helicopter system is considered an excellent candidate for carrying heavy loads or loads of large dimension that are not appropriate for single-helicopter operation, e.g., telephone poles, logs, pipes, trusses, etc.[1] Figure 1 shows one of the most promising of such configurations in which the load is suspended from a spreader bar between the two vehicles. The work reported herein is an analytical extension of the

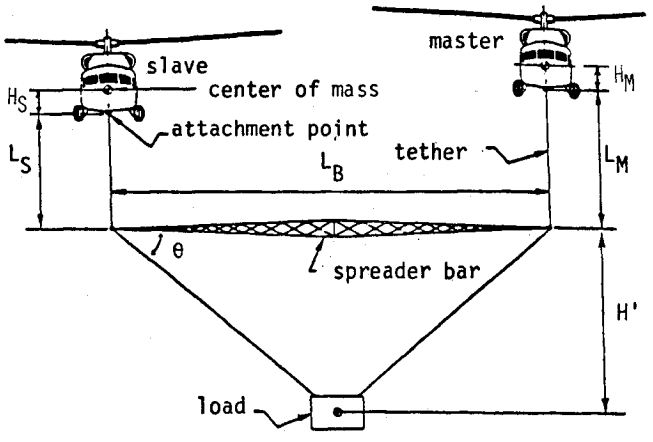

Fig. 1 Twin-lift helicopter configuration (from Ref. 1).

pioneering study of Ref. 1, which analyzed the planar lateral/vertical stability and control characteristics of the twin-lift configuration of Fig. 1. Curtis and Warburton[1] proposed a feedforward control technique in which control movements in the master helicopter were fed directly to the slave vehicle. As analyzed here, the twin-lift configuration also employs a "master/slave" control concept. Here, however, both vehicles are assumed to be under manual control and the translational motion of the "master" helicopter provides a continuous position command to the slave vehicle pilot. Thus, this work is intended to emphasize the manual control aspects of the twin-lift system and to establish plausible manual feedback loop structures and requisite pilot equalization requirements.

System Equations of Motion

Only planar lateral/vertical motion about hover will be considered in this study. In the analysis to follow, it is assumed that the master and slave helicopters are identical. The helicopters and spreader bar are modeled as rigid distributed masses. The slung load is treated as a point mass and all cables are treated as massless rigid links with frictionless attachment points. Only the dominant aerodynamic and propulsive forces and moments acting on the helicopters are included and are introduced in the form of eight stability derivatives. All rotor degrees of freedom are neglected and rotor-induced rolling moments are assumed to be directly proportional to lateral cyclic pitch inputs by the pilot. Collective pitch inputs are assumed to yield instantaneous changes in rotor thrust and no tail rotor effects are considered. These assumptions are identical to those of Ref. 1. Table 1 lists the inertial and aerodynamic characteristics used in the master and slave helicopter models, as well as the nominal characteristics of the remainder of the twin-lift system. The helicopter data are representative of a vehicle the size of the UH-60A.

As modeled here, the twin-lift system possesses seven degrees of freedom defined by the following variables: y_M, y_S, z_M, z_S, ϕ_M, ϕ_S, and ε_B. Figure 2 shows these variable that are the two-position coordinates of the centers of mass of each helicopter, the roll attitude of each vehicle, and the inclination of the spreader bar. A number of related parameters are also shown in the figure.

The equations of motion of the twin-lift system were obtained from Lagrange's equations. The resulting nonlinear equations were then linearized about a condition of steady hovering flight and are

$$m_S\ddot{y}_S + m_B\ddot{y}_B + m_L\ddot{y}_L + m_M\ddot{y}_M + \left(m_S + \frac{m_B+m_L}{2}\right)g\phi_S + \left(m_M + \frac{m_B+m_L}{2}\right)g\phi_M = 0 \tag{1a}$$

$$m_S\ddot{z}_S + m_B\ddot{z}_B + m_L\ddot{z}_L + m_M\ddot{z}_M - F_{\dot{z}_S}\dot{z}_S - F_{\dot{z}_M}\dot{z}_M = F_{\delta_{cS}}\delta_{cS} + F_{\delta_{cM}}\delta_{cM} \tag{1b}$$

$$I_S\ddot{\phi}_S + H_S\left[m_B\ddot{y}_B + m_L\ddot{y}_L + m_M\ddot{y}_M + \frac{m_B+m_L}{2}g\phi_S + \left(m_M + \frac{m_B+m_L}{2}\right)g\phi_M\right] - M_{\dot{\phi}_S}\dot{\phi}_S - M_{\dot{y}_S}\dot{y}_S = M_{\delta_{aS}}\delta_{aS} \tag{1c}$$

$$m_B\ddot{y}_B + m_L\ddot{y}_L + m_M\ddot{y}_M + \frac{m_B+m_L}{2}g\varepsilon_S + \left(m_M + \frac{m_B+m_L}{2}\right)g\phi_M = 0 \tag{1d}$$

$$I_B\ddot{\varepsilon}_B + L_B\left(\frac{m_B}{2}\ddot{z}_B + \frac{m_L}{2}\ddot{z}_L + m_M\ddot{z}_M\right) - F_{\dot{z}_M}\dot{z}_M + H'(m_L\ddot{y}_L + m_Lg\varepsilon_B) = L_BF_{\delta_{cM}}\delta_{cM} \tag{1e}$$

$$m_M\ddot{y}_M - \frac{m_B+m_L}{2}g\varepsilon_M + \left(m_M + \frac{m_B+m_L}{2}\right)g\phi_M = 0 \tag{1f}$$

$$I_M\ddot{\phi}_M - H_M(m_M\ddot{y}_M + m_Mg\phi_M) - M_{\dot{\phi}_M}\dot{\phi}_M - M_{\dot{y}_M}\dot{y}_M = M_{\delta_{aM}}\delta_{aM} \tag{1g}$$

The positions of the master helicopter, spreader bar, and slung load can, of course, be expressed in terms of the dependent variables in Eqs. (1). These are

$$y_M = y_S + H_S\phi_S + L_S\varepsilon_S + L_B - L_M\varepsilon_M - H_M\phi_M \tag{2a}$$

$$z_M = z_S - H_S - L_S + L_B\varepsilon_B + L_M + H_M \tag{2b}$$

$$y_L = y_S + H_S\phi_S + L_S\varepsilon_S + L_B/2 + H'\varepsilon_B \tag{2c}$$

$$z_L = z_S - H_S - L_S + (L_B/2)\varepsilon_B \tag{2d}$$

$$y_B = y_S + H_S\phi_S + L_S\varepsilon_S + L_S/2 \tag{2e}$$

$$z_B = z_S - H_S - L_S + (L_B/2)\varepsilon_B \tag{2f}$$

where $H' = (L_B/2)\tan\theta$.

Equations (1) and (2) constitute the equations of motion of the twin-lift system.

System Stability Characteristics

Reference 1 shows that the assumption of identical helicopter dynamics and equal tether lengths L_M and L_S lead to the definition of a set of generalized coordinates that decouple the seven degrees-of-freedom system into three dynamically inde-

Table 1 Characteristics of twin-lift helicopter system

Helicopter Type	UH-60A
D	52.5 ft
m_H	401.2 slugs
I_H	5629.0 slug·ft^2
m_B	0.118 m_H
m_L	1.06 m_H
H_M,H_S	3.6 ft
L_M,L_S	13.0 ft
L_B	78.75 ft
θ	60 deg
$F_{\delta_{cM}}$,$F_{\delta_{cS}}$	4034.0 lbf/in.
$M_{\delta_{aM}}$,$M_{\delta_{aS}}$	7487.0 ft·lbf/in
$F_{\dot{z}_M}$,$F_{\dot{z}_S}$	− 149.0 lbf·s/ft
$M_{\dot{\phi}_M}$,$M_{\dot{\phi}_S}$	− 20,000.0 lbf·ft·s/rad
$M_{\dot{y}_M}$,$M_{\dot{y}_S}$	232.0 lbf·s

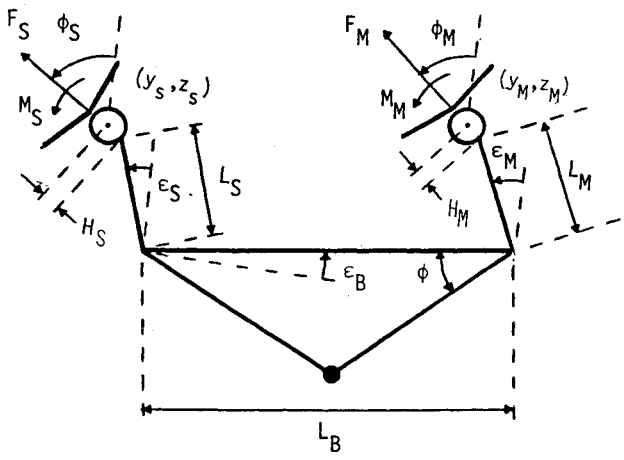

Fig. 2 Coordinate definitions.

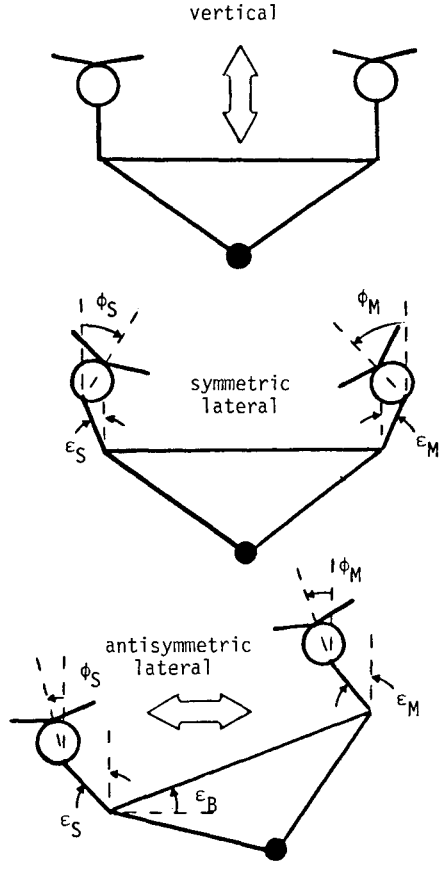

Fig. 3 Mode shapes of three subsystems.

pendent subsystems. Figure 3 (taken from Ref. 1) shows the mode shapes of the three subsystems, called 1) the system of vertical motion, 2) the system of symmetric lateral motion, and 3) the system of antisymmetric lateral motion. Figures 4 and 5 represent a modal analysis of these decoupled systems for the characteristics summarized in Table 1. The reader is referred to the nomenclature list for the definitions of the variables appearing in these figures and in Eqs. (1) and (2). Note the existence of two unstable modes in Figs. 4 and 5, an aperiodic divergence with a real root at $s = 0.761$ (0.91 s time to double amplitude) in the system of symmetric lateral motion, and a periodic divergence associated with a complex pair at $s = 0.72 \pm 0.395j$ (9.6 s time to double amplitude) in the system of antisymmetric lateral motion. The aperiodic divergence associated with the symmetric lateral motion is a static instability wherein helicopter roll and lateral displacements of equal magnitude, but opposite sign, occur. The characteristics of this divergence approximate the characteristics of an inverted pendulum of length L_M or L_S as H_M and H_S become large. The aerodynamic derivatives have little effect on this divergence.[1]

Reference 1 demonstrated the effects of specific parameter variations on the open-loop (uncontrolled) stability of the twin-lift system. These include the effect of tether attachment points H_M and H_S and the load position with respect to the spreader bar H'. The effect of variation in the load size on the symmetric and antisymmetric modal characteristics is also important and is summarized in Figs. 6 and 7. Figure 6 shows that, as the mass ratio m_L/m_H is decreased from the "nominal" value of 1.06 to 0 (no load), the magnitude of the unstable real root and the natural frequency of the oscillatory mode decrease in the symmetric mode. Figure 7 demonstrates that a similar variation in the mass ratio destabilizes both the mid- and high-frequency oscillatory modes, while stabilizing the low-frequency oscillatory pair in the antisymmetric mode. The "no-load" case ($m_L/m_L = 0$) is of more than just academic interest as this condition would occur prior to load-lift-off and after load placement or an emergency release with the vehicles still attached to the spreader bar. The latter condition is of interest from a manual control standpoint as the emergency load release would be instantaneous and potential stability problems could arise if pilot adaptation is required. This subject will be addressed in the next section.

It should be noted that spreader bar length L_B was not a variable in this analysis. Spreader bar lengths of 1.3–2 times the rotor diameter have been proposed and it is usually desired to minimize L_B to minimize the weight of the bar, within safety. The automatic control system analysis of Ref. 1 states that 1.6 rotor diameters was an "optimum" figure. Here, the spreader bar was assumed to be 1.5 rotor diameters in length.

Pilot/Vehicle Analysis of the Twin-Lift System

Figures 8 and 9 illustrate the candidate manual feedback loop closures analyzed in this study. The particular loop closures of Figs. 8 and 9 were chosen since they reflect sound

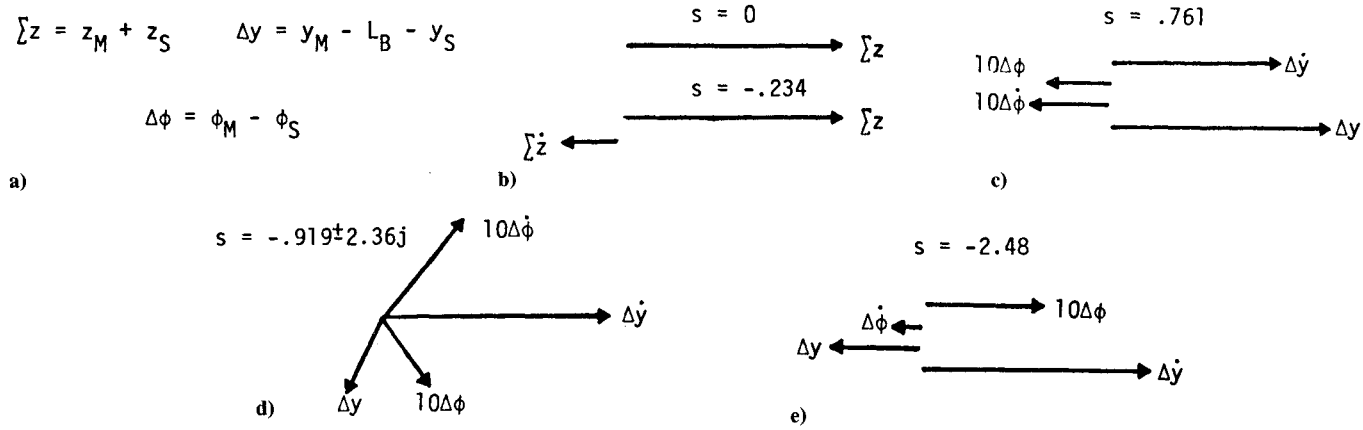

Fig. Phasor diagrams: a) coordinate definitions, b) vertical system, c–e) symmetric lateral system.

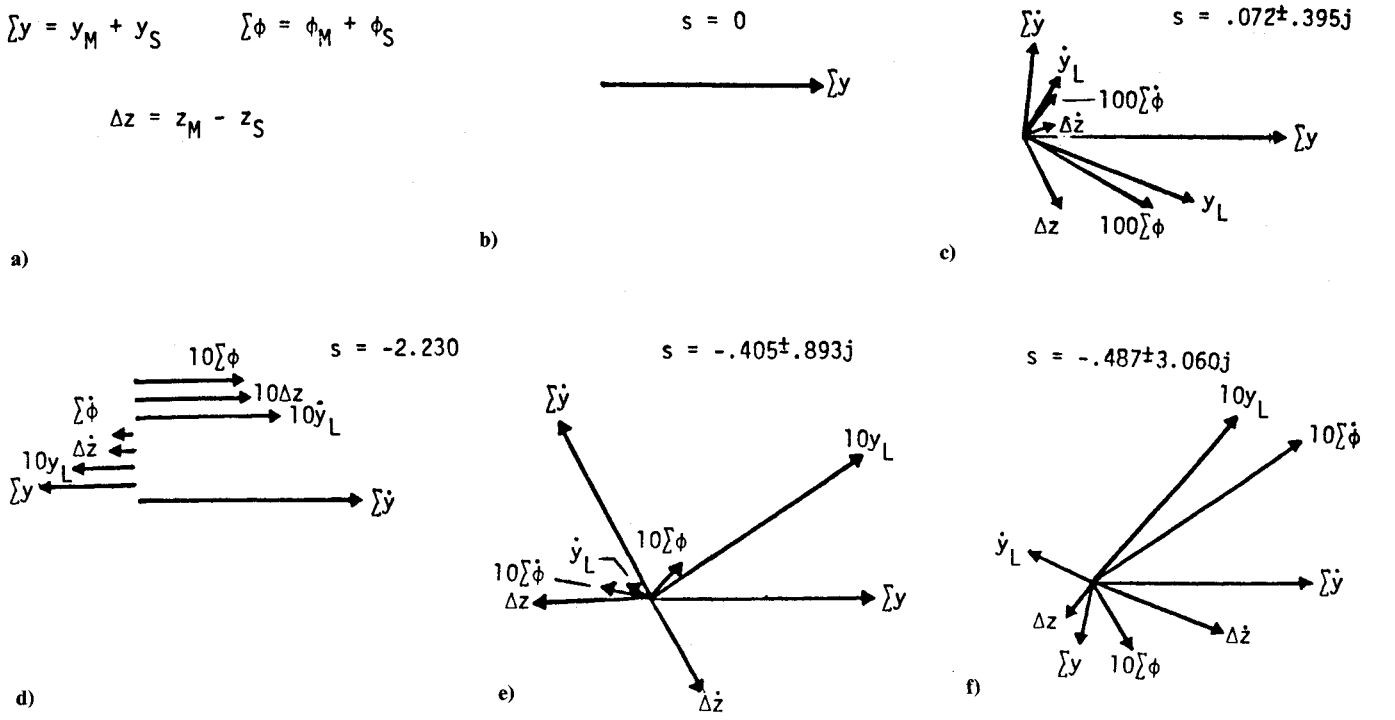

Fig. 5 Phasor diagrams: a) coordinate definitions, b–f) antisymmetric system.

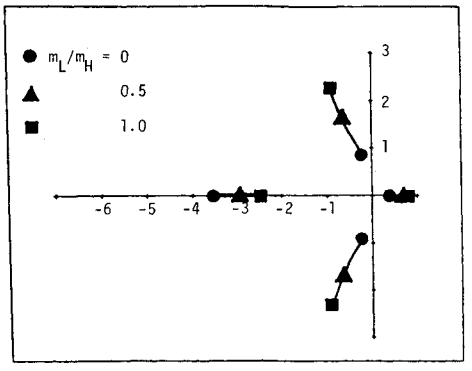

Fig. 6 Effect of slung load size upon symmetric modal characteristics.

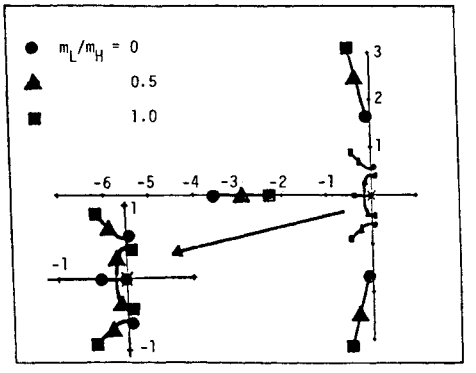

Fig. 7 Effect of slung load size upon antisymmetric modal characteristics.

classical feedback control system design principles and exhibit a feedback structure that has been shown to be valid for single-helicopter hovering flight under manual control.[2] This manual control system differs from the control system developed and analyzed in Ref. 1 in terms of the feedback structure. Reference 1 considered a single pilot flying the master helicopter with his control inputs fed forward to the slave vehicle. Both master and slave vehicles employed attitude feedback stability augmentation systems. In Figs. 8 and 9, a two-pilot manual system is assumed with identical inner feedback loops being closed by both command and slave pilots. In Fig. 8, inner-loop roll attitude feedback (with pilot equalization) is used to provide basic system stabilization and to create improved "effective" vehicle dynamics for the outer-loop lateral closures. In Fig. 9, inner-loop altitude rate feedback is used, with the outer-loop closures employing vertical position errors in a manner completely analogous to the lateral position errors in Fig. 8. For the master pilot, the outer-loop error is the difference between a command vehicle position (presumably generated by the master pilot) and the actual master vehicle position. For the slave pilot, the outer-loop error in the deviation in vehicle separation distance from the nominal. Outer-loop lateral and vertical separation feedback is a reasonable choice given the nature of the task and the visual cues available to the slave helicopter pilot. The acceptability of the loop closures of Figs. 8 and 9 will depend upon the system performance that can be obtained within the limitations imposed by realistic pilot equalization capabilities as discussed in Ref. 3.

The pilot vehicle analysis begins with the assignment of likely manual crossover frequencies for each of the eight feedback loops of Figs. 8 and 9. These were selected as follows:

$$\omega_{c_\phi} = 4.0 \text{ rad/s} \qquad \omega_{c_z} = 2.0 \text{ rad/s}$$
$$\omega_{c_y} = 1.0 \text{ rad/s} \qquad \omega_{c_z} = 0.5 \text{ rad/s} \qquad (3)$$

As can be seen, the crossover frequencies for corresponding loops in the master and slave vehicles are identical and decrease in magnitude as one moves from inner to outer loops. For any pair of serial loop closures, the ratio of inner-to-outer loop crossover frequencies is 4. In addition, the inner-loop altitude rate crossover frequency is a factor of two smaller than the inner attitude loop. Finally, the highest crossover frequency has been selected as 4 rad/s, which represents the upper limit

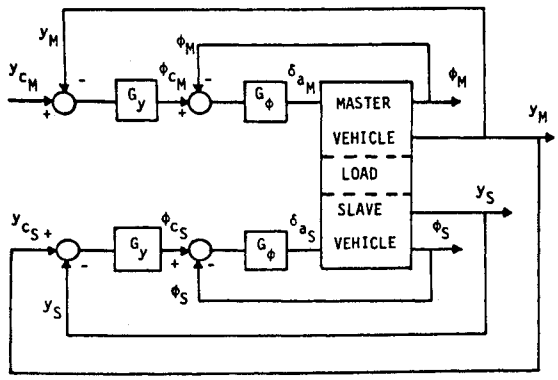

Fig. 8 Loop closures for lateral manual control.

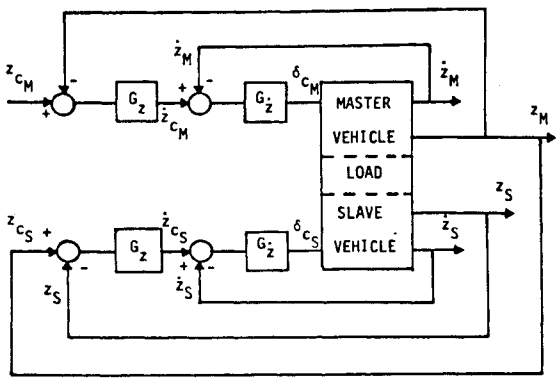

Fig. 9 Loop closures for vertical manual control.

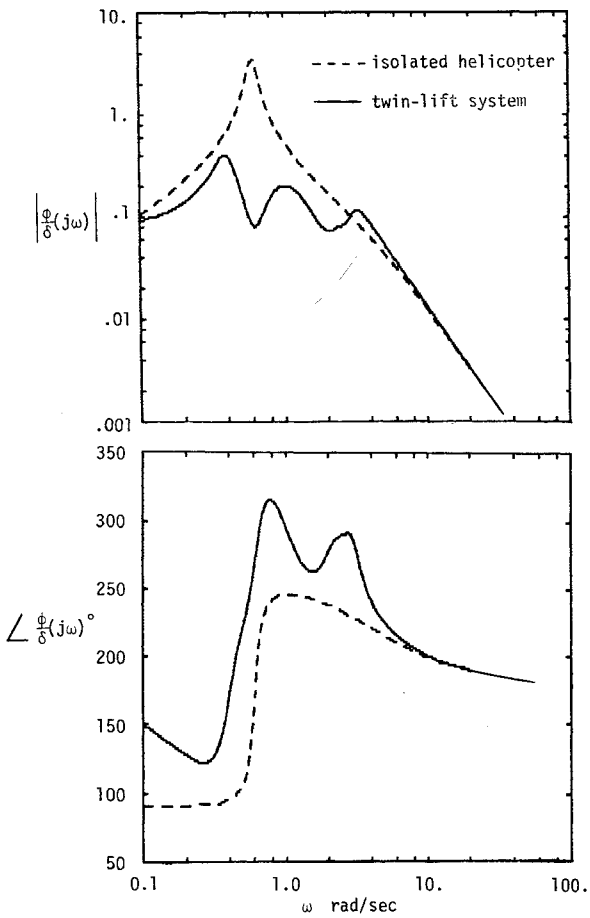

Fig. 10 Roll attitude to lateral cyclic frequency responses for isolated helicopter and one vehicle in twin-lift system.

Table 2 Twin-lift system eigenvalues

Uncontrolled system	Attitude loops closed	All loops closed
0.0	0.0	0.0
0.0	0.0	−0.143
−0.072	−0.107	−0.294 ± 0.794j
0.072 ± 0.395j	−0.234	−1.05
0.761	−0.0825 ± 0.519j	−1.26
−0.405 ± 0.893j	−0.338 ± 598j	−1.06 ± 1.45j
−2.23	−0.297 ± 2.51j	−0.924 ± 2.25j
−2.48	−3.65 ± 1.49j	−4.09
−0.919 ± 2.36j	−3.70 ± 1.41j	−4.82
−0.487 ± 3.06j		−5.05
		−5.62

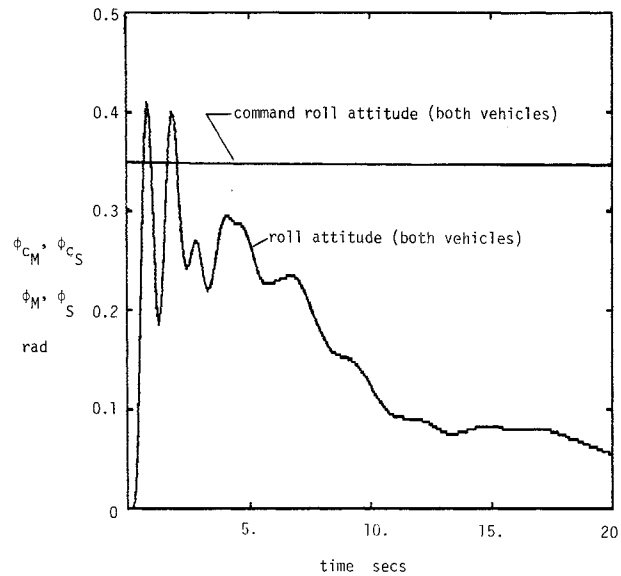

Fig. 11 Roll attitude responses of both helicopters.

for typical compensatory tracking tasks.[3] All these considerations reflect sound manual control system design principles.[4]

After crossover frequency selection, the pilot/vehicle analysis proceeds from the innermost to outermost loop with closures occurring in order of decreasing crossover frequency. First, the pilot equalization for the master helicopter attitude loop is selected by using the crossover model of the human pilot[3] for the crossover frequency ω_{c_ϕ}. With this equalization, the master loop is analytically closed and the pilot equalization for the slave loop is selected, again using the crossover model for the crossover frequency ω_{c_ϕ}. The preceding technique would normally be an iterative process if closure of one of the corresponding loops in master or slave vehicle significantly alters the effective vehicle dynamics in the other vehicle. However, throughout this analysis, it was found that no iterations were required and identical pilot equalization obtained in the first iteration could be used in corresponding loops in master and slave vehicles.

Figure 10 shows a comparison of the roll attitude to lateral cyclic frequency responses for the twin-lift system and the isolated master (or slave) helicopter. It is interesting to compare the probable pilot equalization requirements between the twin-lift system and the isolated helicopter for this, the first of the loop closures in the pilot/vehicle analysis. An application of the crossover model of the human pilot for an attitude-loop crossover frequency of 4 rad/s would require a pilot lead generation of the form

$$G_\phi(s) = 10.0(0.333s + 1) \quad (4)$$

for either system. The higher-order nature of the twin-lift system dynamics as compared to that of the basic helicopter does not yield as broad a k/s-like region for the compensated open-loop; nonetheless, the compensation of Eq. (4) is adequate for the twin-lift roll attitude closure. The lead time constant of 0.333 s does not imply excessive pilot workload, of and by itself.[3] As mentioned above, the equalization of Eq. (4) was acceptable for both master and slave pilot models. What is more important, however, is that when attitude loops of both helicopters were closed with the equalization of Eq. (4) the entire twin-lift system was stabilized. The first two columns of Table 2 show the eigenvalues of the uncontrolled system and the system with both attitude loops closed with the equalization of Eq. (4). It should be noted that while providing basic system stabilization, the attitude closures, themselves, exhibit poor command following characteristics. This is demonstrated in Fig. 11, which shows the attitude responses of the twin-lift system to identical 20 deg roll attitude commands with no other feedback loops closed. This poor command-following response is not surprising, given the higher-order characteristics of the twin-lift frequency response of Fig. 10. As will be seen, however, this command-following performance will be of little consequence in the important position performance of the twin-lift system.

The loop-by-loop analysis technique proceeds until the final manual feedback loop is closed. As one moves from inner to outer loops, the stabilization provided by inner-loop closures causes the "effective" vehicle dynamics to appear to be of lower order than that evident, say, in the twin-lift transfer function of Fig. 10, which was used in the first closure. Such an apparent reduction in system order is a well-known consequence of the loop-by-loop manual control design adopted here in the pilot/vehicle analysis.[5] Figure 12, for example, shows the transfer function $z_M/\dot{z}_{c_M}$ when all but the final altitude loops have been closed by the pilots. This transfer function can, with a fair degree of accuracy, be approximated by

$$\frac{z_M}{\dot{z}_{c_M}}(s) = \frac{0.8}{s(0.25s + 1)} \tag{5}$$

The pilot transfer functions resulting from this analysis are remarkedly simple in form and can summarized as

$$G_\phi(s) = 10.0(0.333s + 1) \qquad G_{\dot{z}}(s) = 0.589$$

$$G_y(s) = -0.0138(1.667s + 1) \quad G_z(s) = 0.546 \tag{6}$$

In keeping with the simplified nature of the system model, no pilot neuromuscular system dynamics (in G_ϕ and $G_{\dot{z}}$) have been considered. However, the effects of effective time delays in these transfer functions will be considered in the computer simulation that is the subject of the next section. The third column of Table 2 shows the eigenvalues of the pilot/vehicle system when all the manual loops have been closed.

In addition to the high-bandwidth attitude control that is essential in stabilizing the entire twin-lift system, the necessity of sensing and utilizing lateral helicopter *separation* rate on the part of the slave pilot defines the workload-intensive elements of the twin-lift flight control task studied herein. The use of separation rate is implied in the slave pilot transfer function in Fig. 8 with $y_{c_S} = y_M$. Sensing this rate would depend exclusively upon visual cues, since slave vehicle motion cues would be of little use as the motion of *both* the slave and master helicopter are involved in defining the vehicle separation. Note that, although the master pilot also uses rate information in closing the lateral displacement loop, it is not the separation rate that is involved, but rather master helicopter lateral velocity relative to an internally generated position command y_{c_M}. The workload associated with roll attitude control can, of course, be ameliorated with stability augmentation, such as that provided by an attitude command/attitude hold system. Indeed, this would probably be a prerequisite to successful

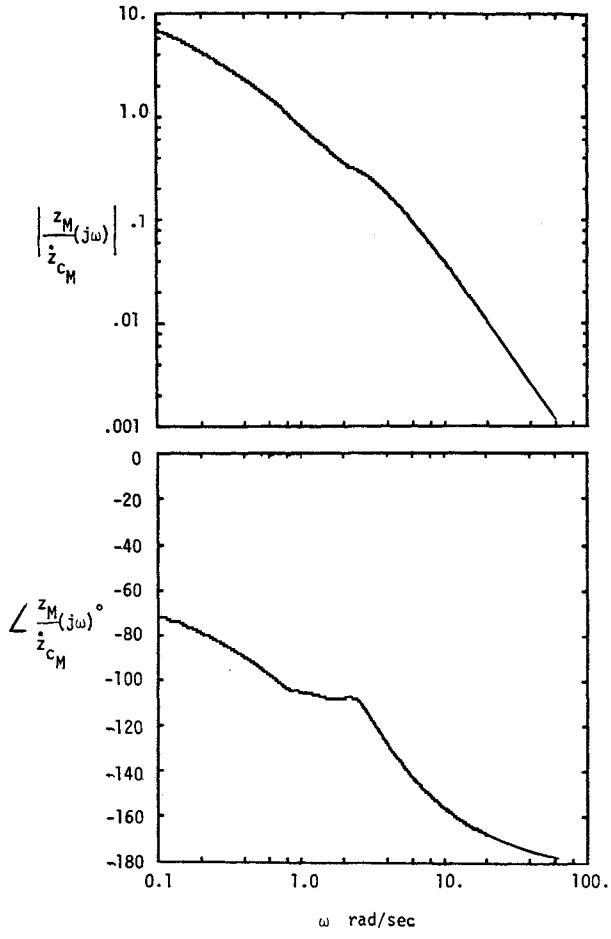

Fig. 12 Altitude to altitude-command frequency response for master vehicle in twin-lift system (all but final altitude loops closed).

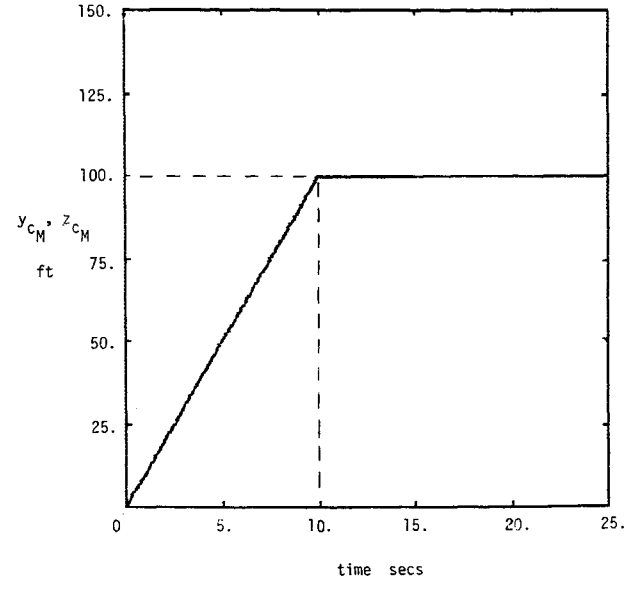

Fig. 13 Twin-lift position commands.

twin-lift operation with tolerable workload. In addition, however, providing a slave helicopter cockpit display of "quickened" lateral separation error is a possibility for additional workload reduction. As a manual control display improvement tool, quickening is a venerable concept.[6] As employed here, it

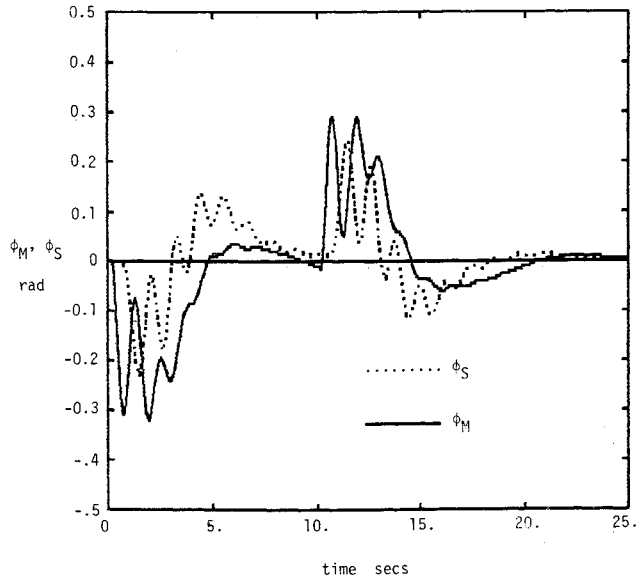

Fig. 14 Roll attitude responses, crossover frequencies of Eq. (3).

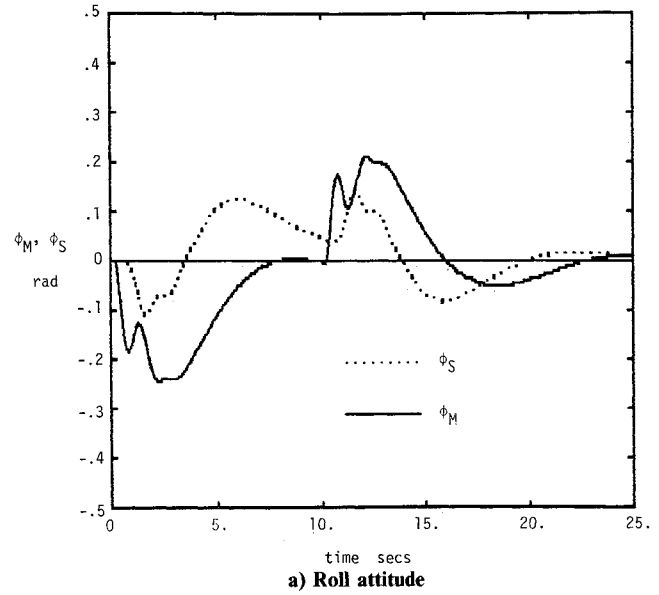

a) Roll attitude

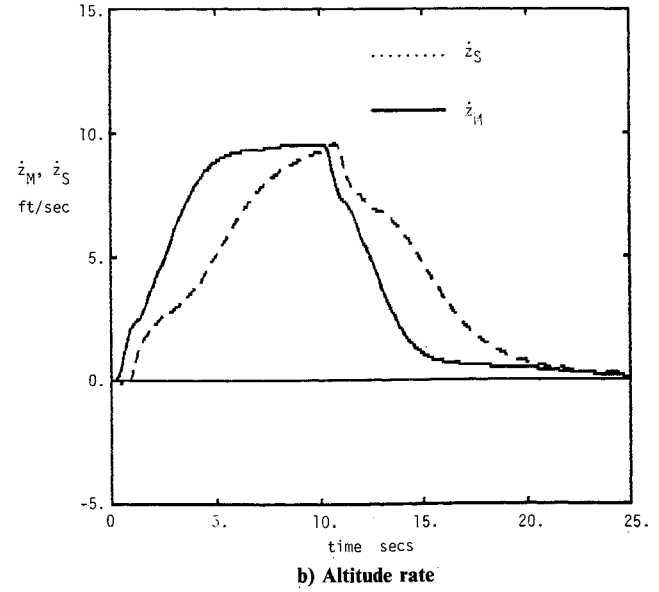

b) Altitude rate

Fig. 15 Inner-loop vehicle responses, reduced crossover frequencies.

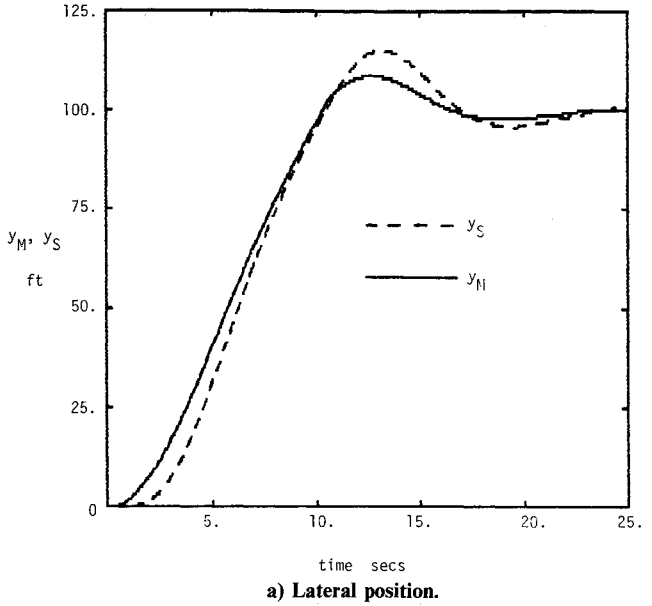

a) Lateral position.

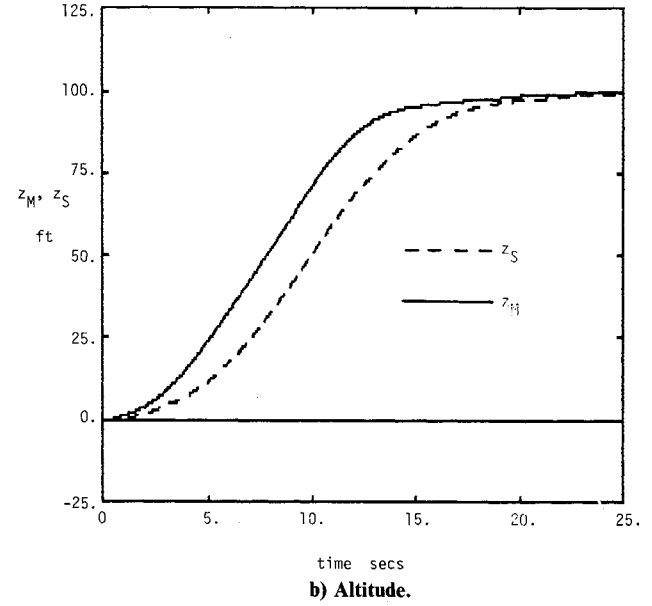

b) Altitude.

Fig. 16 Outer-loop vehicle responses, reduced crossover frequencies.

would entail driving a cockpit display element via the law

$$d_y = K(1.667s + 1)(y_M - y_S) \tag{7}$$

The information necessary for calculating $y_M - y_S$ and its derivative could be obtained by sensing the angles that the tether cables (of unknown length) make with the spreader bar at the attachment points, taking into account the effect of bar inclination due to altitude differences between the master and slave vehicles. This possibility has been discussed in Ref. 1.

Computer Simulation of the Piloted Twin-Lift System

A computer simulation of the twin-lift system incorporating the pilot transfer functions summarized in Eq. (6) was undertaken. An effective time delay of 0.2 s was included in the innermost loop closures defined by G_ϕ and $G_{\dot{z}}$ for both pilots. Simultaneously y_{c_M} and z_{c_M} position commands shown in Fig. 13 were used in the simulation. These signals represent commanded position changes obtained at nominal translation rates of 10 ft/s. Outer-loop position responses of the twin-lift system to these commands were excellent, however, the roll attitude responses, shown in Fig. 14, were somewhat oscillatory. This

can be attributed to the relatively high roll attitude crossover frequency of 4.0 rad/s adopted in the pilot/vehicle analysis. It was felt that the roll oscillations would not be tolerated by actual pilots. Hence, the crossover frequencies of all loop closures were reduced to 75% of the values shown in Eq. (3). This meant a commensurate 25% reduction of the gains in the pilot transfer functions shown in Eq. (6). The resulting twin-lift system performance is summarized in Figs. 15 and 16. The outer-loop performance is excellent and the vehicle roll attitude responses are much less oscillatory than those in Fig. 14.

When the position commands of Fig. 13 were employed with no load and with the reduced gain pilot models, the twin-lift system was unstable. An increase in pilot gains to the values of Eq. (6), however, stabilized the system and overall system performance was excellent, including roll attitude responses. This suggests that pilot adaptation in the form of gain adjustment is necessary in going from a load to a no-load condition or vice versa.

Conclusions

1) The basic pilot equalization requirements for manual twin-lift helicopter operation in a task of lateral/vertical hovering flight have been established. The analysis methodology was based upon a classical frequency domain technique utilizing the crossover model of the human pilot. The feedback structure which was chosen was similar to that which has been used in pilot/vehicle analyses of isolated hovering helicopters.

2) In addition to the high-bandwidth roll attitude control essential for stabilizing the entire twin-lift system, the necessity of sensing and utilizing lateral helicopter separation rate on the part of the slave pilot defines the workload intensive elements of the flight control task studied here.

3) An attitude command/attitude hold stability and command augmentation system may well be a necessity for twin-lift operation with tolerable workload. In addition, the inclusion of a cockpit display of quickened lateral separation error may be of use to the pilot of the slave helicopter.

Acknowledgment

Data on the basic geometry and loading for the twin-lift/spreader bar helicopter system were provided by Mr. Luigi S. Cicolani of the Flight Dynamics and Controls Branch of NASA Ames Research Center. His assistance in the initiation of this study is gratefully acknowledged.

References

[1]Curtis, H. C. Jr. and Warburton, F. W., "Stability and Control of the Twin-Lift Helicopter System," *Journal of the American Helicopter Society*, April 1985, Vol. 30, pp. 14–23.

[2]Heffley, R. K., "A Compliation and Analysis of Helicopter Handling Qualities Data, Vol. II: Data Analysis," NASA CR-3144, Aug. 1979.

[3]McRuer, D. T. and Krendel, E. S., "Mathematical Models of Human Pilot Behavior," AGARDograph AG-188, Jan. 1974.

[4]Hess, R. A., "Feedback Control Models," *Handbook of Human Factors*, edited by G. Salvendy, Wiley, New York, 1986. Chap. 9.5, pp. 1212–1242.

[5]McRuer, D. T., Graham, D., and Ashkenas, I., *Aircraft Dynamics and Automatic Control*, Princeton University Press, Princeton, NJ, 1972.

[6]Birmingham, H. P. and Taylor, F. V., "A Design Philosophy for Man-Machine Control Systems, *Proceedings of the IRE*, Vol. 42, Dec. 1954, pp. 1748–1758.